Supplementary Information

Single-Shot Replica-Free Common-Path Quantitative Phase Imaging with Doubled Field of View

Aleksandra Piekarska [1], Mikołaj Rogalski [1], Marzena Stefaniuk [2], Maciej Trusiak [1], Piotr Zdańkowski [1*]

[1] Institute of Micromechanics and Photonics, Warsaw University of Technology, Warsaw, 02-525, Poland

[2] Laboratory of Neurobiology, BRAINCITY, Nencki Institute of Experimental Biology of Polish Academy of Sciences, Warsaw, 02-093, Poland

[*]Correspondence: piotr.zdankowski@pw.edu.pl

Supplementary Note 1

Description of the GDRS algorithm implementation

The GDRS algorithm is an iterative optimization method designed to reconstruct and separate two independent phases, φ_{+1} and φ_{-1}, from a series of $N \geq 2$ overlapped phase images acquired from a common-path shearing digital holographic microscope ($\varphi_{\pm 1}$). Importantly, each overlapped phase image must be acquired with different spatial separation ($\Delta\mathbf{r} = (\Delta x, \Delta y)$) of subsequent n-th images, so that:

$$\varphi_{\pm 1}(\mathbf{r}, n) = \varphi_{+1}\big(\mathbf{r} + \Delta\mathbf{r}(n)\big) - \varphi_{-1}\big(\mathbf{r} - \Delta\mathbf{r}(n)\big), \quad \text{Eq. (S1)}$$

where $\mathbf{r} = (x, y)$ represents the spatial coordinates of the 2D phase distribution.

The proposed algorithm leverages a forward model from Eq. (S1) and predefined spatial shifts $\Delta\mathbf{r}(n)$ to iteratively minimize the estimation error using a gradient descent approach. The algorithm, which pseudocode is shown in Algorithm S1, begins by establishing an initial guess for the separated phases. The initial estimate for the positive phase, $\varphi_{+1}(\mathbf{r})$, is constructed by shifting each observation by $-\Delta\mathbf{r}(n)$ and computing the maximum projection across all N frames. Analogously, the negative phase, $\varphi_{-1}(\mathbf{r})$, is initialized by shifting the inverted observations by $+\Delta\mathbf{r}(n)$ and taking the maximum. This provides a robust, data-driven starting point for the optimization.

After the initialization, the iterative optimization begins. For each iteration m up to M_{iter}, the algorithm processes all N overlapped phases sequentially to update the phase estimates. Firstly, an estimate of the n-th observation, $\varphi_{\pm 1}^{est}(\mathbf{r}, n)$, is generated by shifting the current estimates of $\varphi_{+1}(\mathbf{r})$ and $\varphi_{-1}(\mathbf{r})$ according to the mathematical forward model (Eq. S1) governing the physical system. Next, the estimation error, $\nabla\varphi_{\pm 1}(\mathbf{r}, n)$, is computed as the difference between the forward model prediction and the actual measured data. Subsequently, the calculated residual is propagated back into the coordinate space of the individual phases. The shifts applied here are the exact inverses of those used in the forward model, aligning the error with the spatial domain of $\varphi_{+1}(\mathbf{r})$ and $\varphi_{-1}(\mathbf{r})$. Finally, the separated phases are updated using the gradient descent rule. The estimates are adjusted proportionally to the backpropagated error scaled by the learning rate α.

In our practical implementation, the learning rate was set α to 0.1 for all reconstructions. We empirically observed that this value yields robust results across all investigated cases; a larger α could cause the algorithm to diverge, whereas a smaller value resulted in unnecessarily slow convergence. The total number of iterations, M_{iter}, was fixed at 20 for all scenarios, as any subsequent iterations produced only negligible reductions in the reconstruction error. Furthermore, to mitigate the risk of converging to local minima, the indices n of the input observations were randomly reshuffled at the beginning of each global iteration m.

	GDRS algorithm
	Inputs: $\varphi_{\pm 1}(\mathbf{r}, n)$; $\Delta\mathbf{r}(n)$; M_{iter}; α **Outputs:** $\varphi_{+1}(\mathbf{r})$; $\varphi_{-1}(\mathbf{r})$
	% Initial guess of separated phases

$$\varphi_{+1}(\mathbf{r}) = \max_{1\le n\le N}\left(\varphi_{\pm1}(\mathbf{r}-\Delta\mathbf{r}(n),n)\right)$$
$$\varphi_{-1}(\mathbf{r}) = \max_{1\le n\le N}\left(-\varphi_{\pm1}(\mathbf{r}+\Delta\mathbf{r}(n),n)\right)$$
for: $m = 1: M_{iter}$

  for: $n = 1: N$

  % Forward model – estimate $\varphi_{\pm1}$ from φ_{+1} and φ_{-1}
$$\varphi^{est}_{\pm1}(\mathbf{r},n) = \varphi_{+1}(\mathbf{r}+\Delta\mathbf{r}(n)) - \varphi_{-1}(\mathbf{r}-\Delta\mathbf{r}(n))$$
  % Calculate the estimation error
$$\nabla\varphi_{\pm1}(\mathbf{r},n) = \varphi^{est}_{\pm1}(\mathbf{r},n) - \varphi_{\pm1}(\mathbf{r},n)$$
  % Backward model – propagate error back to φ_{+1} and φ_{-1}
$$\nabla\varphi_{+1}(\mathbf{r}) = \nabla\varphi_{\pm1}(\mathbf{r}-\Delta\mathbf{r}(n),n)$$
$$\nabla\varphi_{-1}(\mathbf{r}) = \nabla\varphi_{\pm1}(\mathbf{r}+\Delta\mathbf{r}(n),n)$$
  % Update the separated phases
$$\varphi_{+1}(\mathbf{r}) = \varphi_{+1}(\mathbf{r}) - \alpha\cdot\nabla\varphi_{+1}(\mathbf{r})$$
$$\varphi_{-1}(\mathbf{r}) = \varphi_{-1}(\mathbf{r}) + \alpha\cdot\nabla\varphi_{-1}(\mathbf{r})$$

Evaluation of the GDRS algorithm under elevated noise conditions

The ability of the algorithms to average noise under elevated noise conditions was investigated experimentally. For this purpose, an additional experiment was performed in which a phase calibration target (Lyncee Tec, Borofloat 33 glass with etched structures of 125 nm height) was imaged through a contaminated coverslip. The presence of the coverslip introduced additional speckle noise in the focal plane, significantly degrading the signal-to-noise ratio. Imaging was performed using a 5×/0.12 microscope objective, and both measurement series were reconstructed using the GDRS algorithm. In the first measurement series, the shift parameter τ was varied by translating the diffraction grating (PG2) along the optical axis with a step size of δ=0.5 mm while maintaining a constant illumination wavelength of λ=535 nm. In the second series, the shift parameter τ_λ was varied by changing the illumination wavelength over the range of 490–585 nm with a spectral step of Δλ=5 nm.

The obtained results are presented in Figure 1. The phase standard deviation (STD) was calculated for object-free regions in each reconstructed phase map. For reference, the STD values under standard noise conditions were taken from the experiment described in Section 2.2.1 of the main manuscript. The corresponding reconstructions and the regions used for STD calculation are shown in Figure 3 of the main manuscript. As indicated by the phase STD values summarized in Table 1, the wavelength-scanning mode enabled more effective averaging of these disturbances.

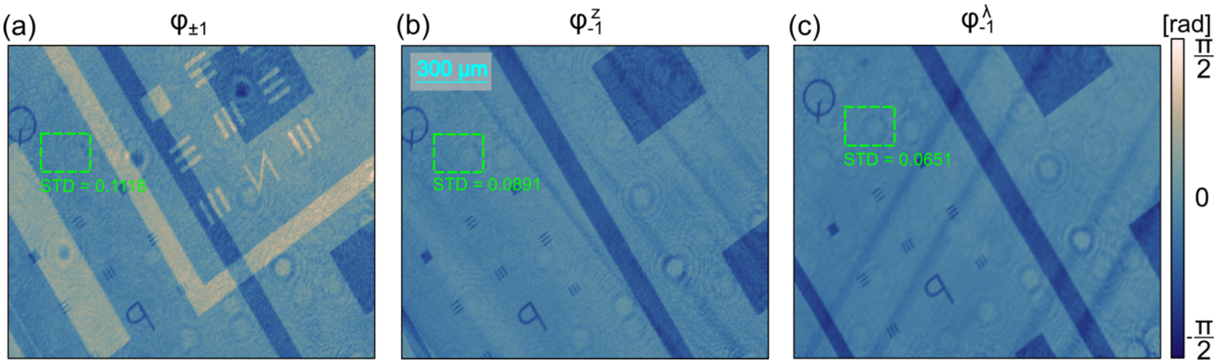

Fig. S1 | Comparison of noise levels after applying grating-shift scanning and wavelength scanning. (a) Phase reconstruction obtained using the FTM. (b)–(c) Phase reconstructions of a single field of view for the grating-shift scanning and wavelength-scanning methods, respectively.

Table 1 Phase standard deviation values of the single frame ($\varphi_{\pm1}$) and the final reconstruction (φ_{-1}) at low and high noise levels

	Standard noise level data	Noisy data
Single phase image $\varphi_{\pm1}$ [rad]	0.0395	0.1118
φ_{-1} R2D-QPI [rad]	0.0178	0.0891
φ_{-1} wsR2D-QPI [rad]	**0.0116**	**0.0651**

Supplementary Note 2

Investigation of the influence of the spectral range on imaging

The influence of the choice of the central wavelength on the reconstruction was investigated experimentally. Figure 2 presents the reconstruction results obtained using the GDRS algorithm for three data series corresponding to different spectral ranges: 420–515 nm (Figure 2(a)), 490–585 nm (Figure 2(b)), and 555–650 nm (Figure 2(c)). Each series comprised $N = 20$ frames, recorded after changing the wavelength, with a step of $\Delta\lambda = 5$ nm between consecutive frames. The focus of the imaging system was set for the central wavelength in each series. The phase reconstructions $\varphi_{\pm 1}$, obtained exclusively from the first frame of each series before the proposed chromatic aberration correction, are shown in Figures 4(a1)–4(c1), and after the correction in Figures 2(a2)–2(c2). Figures 2(a3)–2(c3) show the final reconstructions of the phase φ_{-1}. Despite the identical spectral spacing between the first and the central frame of each series, the object is most strongly defocused for the spectral range containing the shortest wavelengths (Figure 2(a1)). This is caused by the higher steepness of the objective dispersion curve in this range, which results in the same wavelength difference producing a larger change in the refractive index and, consequently, a more pronounced defocus effect. After numerical correction within the proposed GDRS algorithm (Figure 2(a2)), this effect is compensated and the final phase φ_{-1} is reconstructed without defocus aberration (Figure 2(a3)). This enables the use of shorter wavelengths, which provide better resolution, without the risk of image degradation caused by dispersion, since its influence is corrected algorithmically.

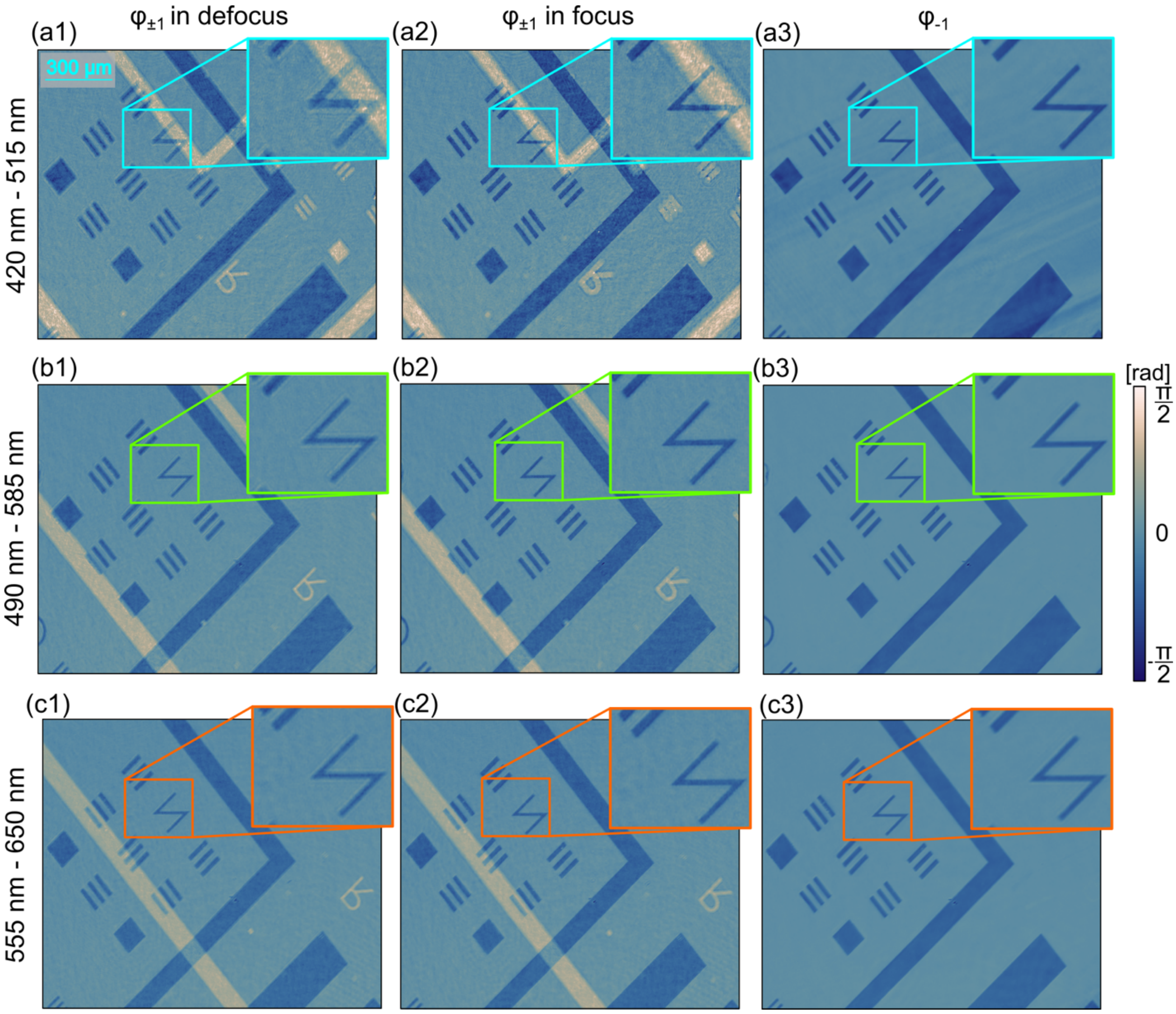

Fig. S2 | Comparison of phase-imaging results obtained for a phase resolution target from image series ($N = 20$) acquired over different illumination wavelength ranges. Phase reconstructions $\varphi_{\pm 1}$ retrieved using the FTM are shown for holograms before propagation to the object plane in (a1)–(c1) and for holograms after propagation to the focal plane in (a2)–(c2). The corresponding reconstructed φ_{+1} and φ_{-1} phase distributions are presented in (a3)–(c3). Results are shown for the following wavelength ranges: (a) 420–515 nm, (b) 490–585 nm, and (c) 555–650 nm.